EJN fens EUROPEAN JOURNAL OF NEUROSCIENCE

European Journal of Neuroscience, Vol. 29, pp. 1287–1293, 2009 doi:10.1111/j.1460-9568.2009.06673.x

COGNITIVE NEUROSCIENCE

The neuroanatomy of grapheme–color synesthesia

Lutz Jäncke, Gian Beeli, Cornelia Eulig and Jürgen Hänggi
Division Neuropsychology, Institute of Psychology, University of Zurich, Binzmuhlestrasse 14, 8050 Zurich, Switzerland

Keywords: diffusion tensor imaging, synesthesia, voxel based morphometry

Abstract

Grapheme–color synesthetes perceive particular colors when seeing a letter, word or number (grapheme). Functional neuroimaging studies have provided some evidence in favor of a neural basis for this type of synesthesia. Most of these studies have reported extra activations in the fusiform gyrus, which is known to be involved in color, letter and word processing. The present study examined different neuroanatomical features (i.e. cortical thickness, cortical volume and cortical surface area) in a sample of 48 subjects (24 grapheme–color synesthetes and 24 control subjects), and revealed increased cortical thickness, volume and surface area in the right and left fusiform gyrus and in adjacent regions, such as the lingual gyrus and the calcarine cortex, in grapheme–color synesthetes. In addition, we set out to analyze structural connectivity based on fractional anisotropy (FA) measurements in a subsample of 28 subjects (14 synesthetes and 14 control subjects). In contrast to the findings of a recent neuroanatomical study using modern diffusion tensor imaging measurement techniques, we did not detect any statistically significant difference in FA between synesthetes and non-synesthetes in the fusiform gyri. Our study thus supports the hypothesis of local anatomical differences in cortical characteristics in the vicinity of the V4 complex. The observed altered brain anatomy in grapheme–color synesthetes might be the anatomical basis for this particular form of synesthesia but it is also possible that the detected effects are a consequence (rather than the primary cause) of the life-long experience of grapheme–color synesthesia.

Introduction

Synesthesia is a perceptual phenomenon in which certain stimuli elicit a sensation in two or more sensory modalities; for example, specific tones may automatically evoke the perception of particular colors. There are different kinds of linkages between sensory modalities, the most frequent being linkages of letters and digits (graphemes) with colors (Rich *et al.*, 2005). The cause of this extraordinary phenomenon is still unknown.

Hubbard & Ramachandran (2005) and Hubbard (2007) proposed an influential two-stage model for the so called grapheme–color synesthesia, one of the most studied variants of synesthesia. According to their model, synesthetic experience arises from abnormal cross-activation between the grapheme area and the color area in the fusiform gyrus (FG) due to synesthesia-specific local connections. The synesthetic color perceptions driven by the FG are then thought to be bound together by top-down mechanisms controlled by the parietal cortex, this in turn resulting in a kind of 'hyperbinding'. This two-stage model was developed on the basis of several studies that reported neuronal correlates for grapheme–color synesthesia (Nunn *et al.*, 2002; Rich & Mattingley, 2002; Hubbard & Ramachandran, 2005; Hubbard *et al.*, 2005a,b; Weiss *et al.*, 2005; Esterman *et al.*, 2006; Sperling *et al.*, 2006; Muggleton *et al.*, 2007; Beeli *et al.*, 2008).

In functional neuroimaging experiments based on functional magnetic resonance imaging and positron emission tomography, specific brain areas have been found to show different activations in grapheme–color or colored-hearing synesthetes compared with controls (Nunn *et al.*, 2002; Rich & Mattingley, 2002; Hubbard & Ramachandran, 2005; Hubbard *et al.*, 2005a; Sperling *et al.*, 2006). Different activations have been found in the left and right color center within the FG (the V4 complex), in the posterior inferior temporal gyrus, in the lingual gyrus, in frontal brain areas and in regions in the (mostly left) parietal cortex (intraparietal sulcus; IPS; Hubbard *et al.*, 2005a,b; Hubbard & Ramachandran, 2005; Weiss *et al.*, 2005; Sperling *et al.*, 2006; Beeli *et al.*, 2008). In addition, inhibition of the right (but not the left) parietal cortex with transcranial magnetic stimulation was found to transiently disrupt synesthesia (Esterman *et al.*, 2006; Muggleton *et al.*, 2007). Different intracerebral activations in these regions have also been reported for synesthetes on the basis of electrical tomography (Beeli *et al.*, 2008).

While these studies support the hypothesis that the identified brain regions are differently involved in the processing of perceived stimuli in synesthetes, a recent paper (Rouw & Scholte, 2007) using diffusion tensor imaging (DTI) provided the first evidence for specific neuroanatomical features in synesthetes. This study demonstrated increased structural connectivity in temporo-occipital, parietal and superior frontal regions in grapheme–color synesthetes, thus supporting the hypotheses of anatomical hyperconnectivity in grapheme–color synesthetes. We recently used voxel-based morphometry and DTI to investigate the neuroanatomical underpinnings of interval–taste and tone–color synesthesia in the multiple synesthete E.S. This case study revealed hyperconnectivity of auditory to gustatory areas and gray and white matter volumetric alterations as well as increased fractional anisotropy (FA) in auditory, gustatory and visual areas (Hänggi *et al.*, 2008). Most recently, Weiss & Fink (2008)

Correspondence: Professor Dr Lutz Jäncke, as above.
E-mail: l.jaencke@psychologie.uzh.ch

Received 16 October 2008, revised 7 January 2009, accepted 20 January 2009

© The Authors (2009). Journal Compilation © Federation of European Neuroscience Societies and Blackwell Publishing Ltd

demonstrated increased GM volumes in the right FG and the left IPS in grapheme–color synesthetes. The preceding findings have been taken as evidence for the Hubbard & Ramachandran (2005) two-stage model of grapheme–color synesthesia.

In the present study we aimed to replicate the preceding anatomical studies and to extend the focus of our study to other anatomical features. In particular, we sought to examine cortical volume, cortical thickness and cortical surface area on the basis of T1-weighted magnetic resonance images in synesthetes and non-synesthetes using well-validated surface-based morphometric methods (Dale *et al.*, 1999; Fischl *et al.*, 1999a; Fischl & Dale, 2000; Kuperberg *et al.*, 2003; Rauch *et al.*, 2004; Salat *et al.*, 2004). We anticipated group differences in brain areas associated with the analyses of colors and graphemes, that is, the FG and adjacent brain regions in the ventral visual stream (Bartels & Zeki, 2000; Pernet *et al.*, 2005; Joseph *et al.*, 2006; Vinckier *et al.*, 2007). In addition, we tested whether superior frontal (as in Rouw & Scholte, 2007) and parietal (as in Rouw & Scholte, 2007; and Weiss & Fink, 2008) brain regions show differences in terms of cortical thickness, cortical volume, cortical surface area and fractional anisotropy.

Materials and methods

Subjects

Twenty-four synesthetes (20 women and four men) with a mean ± SD age of 29.2 ± 10.1 years and 24 controls (20 women and four men; mean age 27.3 ± 6.2 years) matched for age, sex, handedness and education participated in the study. In 28 out of the 48 participants (14 synesthetes and 14 controls) diffusion-weighted images were available (synesthetes, 28.6 ± 7.6 years, 10 women and four men; controls, 29.4 ± 10.4 years, 10 women and four men). With respect to education, most of the participants in both groups have an academic background and hence their years of education are closely matched. Four synesthetes had already participated in our previous investigations (Beeli *et al.*, 2007, 2008). All synesthetes reported a lifelong history of grapheme–color perception (i.e. as long as they could remember) and were tested carefully for their color perception to letters and numbers with the established 'test of genuineness' that is typically used for the diagnosis of synesthesia (Baron-Cohen *et al.*, 1987). All synesthetes had to repeat this test at least 1 month later, and all synesthetes demonstrated constant synesthetic perception. All participants were consistently right handed according to the procedure proposed by Annett (1970), had no history of neurological, neuropsychological or psychiatric disease, and denied taking illegal drugs or medication. The local ethics committee (Kantonale Ethikkommission Zürich, according to the Declaration of Helsinki) approved the study and written informed consent was obtained from all participants.

Magnetic resonance imaging (MRI) data acquisitions

MRI scans were acquired on a 3.0 T Philips Intera whole-body scanner (Philips Medical Systems, Best, The Netherlands) equipped with a transmit–receive body coil and a commercial eight-element sensitivity encoding (SENSE) head coil array. A volumetric 3-D T1-weighted gradient echo sequence (turbo field echo) scan was obtained from all 48 participants, with a measured spatial resolution of $1 \times 1 \times 1.5$ mm^3 (acquisition matrix 224×224 pixels, 180 slices) and a reconstructed resolution of $0.86 \times 0.86 \times 0.75$ mm^3 (reconstructed matrix 256×256 pixels, 180 slices). Further imaging parameters were: Field of view (FOV) = 220×220 mm^2, echo-time (TE) = 2.3 ms, repetition-time (TR) = 20 ms, flip-angle = 20°.

As one aim of the present study was the replication of the findings on structural connectivity by Rouw & Scholte (2007), we adhered as closely as possible to their analysis. Structural connectivity was based on the FA, which was calculated based on diffusion-weighted spin-echo echo-planar imaging measurements (TR = 10,166 ms, TE = 50 ms, flip angle = 90°, FOV = 200 × 200 mm, measured spatial resolution of $2.08 \times 2.13 \times 2.0$ mm^3, matrix size = 96 × 96, 50 slices, slice thickness = 2 mm, reconstructed voxel size = $1.56 \times 1.56 \times 2$ mm^3, reconstructed matrix = 128 × 128 pixels, 50 slices, SENSE factor = 2.1). Diffusion was measured in 15 non-collinear directions with a b-value of 1000 s/mm^2 followed by a non-diffusion-weighted volume (reference volume).

Surface-based morphometry

Cortical surface reconstruction and volumetric segmentation was performed with the FreeSurfer image analysis suite, which is documented and freely available for download online (http://surfer.nmr.mgh.harvard.edu/). The technical details of these procedures are described in prior publications (Dale *et al.*, 1999; Fischl *et al.*, 1999a,b, 2001, 2002, 2004a,b; Fischl & Dale, 2000; Ségonne *et al.*, 2004). Briefly, the 3-D structural T1-weighted MRI scan was used to construct models of each subject's cortical surface in order to measure brain features such as cortical thickness, cortical surface area and cortical volume. This is a fully automated procedure involving segmentation of the cortical white matter (Dale *et al.*, 1999), tessellation of the grey–white matter junction, inflation of the folded surface tessellation patterns (Fischl *et al.*, 1999a) and automatic correction of topological defects in the resulting manifold (Fischl *et al.*, 2001). This surface was then used as the starting point for a deformable surface algorithm designed to find the grey–white and pial (grey matter–cerebrospinal fluid) surfaces with submillimeter precision (Fischl & Dale, 2000). The procedures for measuring cortical thickness have been validated against histological analysis (Rosas *et al.*, 2002) and manual measurements (Kuperberg *et al.*, 2003; Salat *et al.*, 2004). This method uses both intensity and continuity information from the surfaces in the deformation procedure in order to be able to interpolate surface locations for regions in which the MRI image is ambiguous (Fischl & Dale, 2000). For each subject, cortical thickness of the cortical ribbon was computed on a uniform grid (comprised of vertices) with 1 mm spacing across both cortical hemispheres, with the thickness being defined by the shortest distance between the grey–white and pial surface models. The thickness maps produced are not limited to the voxel resolution of the image and are thus sensitive to detecting submillimeter differences between groups (Fischl & Dale, 2000). Thickness measures were mapped to the inflated surface of each participant's brain reconstruction, allowing visualization of data across the entire cortical surface (i.e. gyri and sulci) without being obscured by cortical folding. Each subject's reconstructed brain was then morphed to an average spherical surface representation that optimally aligned sulcal and gyral features across subjects (Fischl *et al.*, 1999b). This procedure provides accurate matching of morphologically homologous cortical locations among participants on the basis of each individual's anatomy while minimizing metric distortions. This transform was used to map the thickness measurements into a common spherical coordinate system. Additionally, parcellation of the cerebral cortex into units based on gyral and sulcal structure (Fischl *et al.*, 2004b; Desikan *et al.*, 2006) and creation of a variety of surface based data including maps of cortical volume and surface area as well as curvature and sulcal depth. Data were resampled for all subjects into a common spherical coordinate system (Fischl *et al.*, 1999b). The data were then smoothed

© The Authors (2009). Journal Compilation © Federation of European Neuroscience Societies and Blackwell Publishing Ltd

on the surface tessellation using an iterative nearest-neighbor averaging procedure (50 iterations were applied, equivalent to applying a two-dimensional Gaussian smoothing kernel along the cortical surface with a full-width-at-half-maximum of ∼13 mm). In addition, we calculated global anatomical measures (cortical volume, cortical thickness and cortical surface area) for each hemisphere in order to use these values as covariates of interest and to control for global between-group differences.

Analysis of FA

Here we applied the preprocessing and analysis of Tract-Based Spatial Statistics (TBSS) (Smith *et al.*, 2006) using FSL (FMRIB Software Library; http://www.fmrib.ox.ac.uk/fsl/) (Smith *et al.*, 2004) tools such as the FDT (FMRIB Diffusion Toolbox) (Behrens *et al.*, 2003) tool to create FA maps. The following steps were realized. (i) Eddy current and head movement correction were applied using the EDDY_CORRECT tool of FDT. (ii) An individual binary brain mask was created on the non-diffusion-weighted images using BET (Brain Extraction Tool). (iii) Tensors were fitted to the data using the DTIFIT toll of FDT. (iv) Non-linear normalization of the FA maps and non-linear registration into a standard stereotactic space was done with TBSS scripts (Smith *et al.*, 2006) implemented in FSL (Smith *et al.*, 2004). (v) Voxel-wise statistical analysis of the FA maps was carried out using TBSS scripts. (vi) A mean FA image was created after alignment into a common stereotactic space and was then reduced to an image called 'mean FA skeleton' (an alignment-invariant tract representation), helping to overcome the problem of the arbitrariness of smoothing extent. (vii) The significance of the comparison between the two groups was calculated by means of voxel-wise *t*-tests for independent comparisons.

Statistical analyses

General linear models were applied to the surface-based morphometric maps and to the FA maps. We compared synesthetes and controls with respect to (i) regional cortical volume; (ii) regional cortical thickness and (iii) regional cortical surface area, while simultaneously controlling for (a) the whole cortical volume; (b) the mean cortical thickness and (c) the whole cortical surface area, respectively. Hemisphere-specific group effects on these latter-mentioned global measurements (a, b and c) as well as on intracranial volume (ICV) were evaluated in addition. In terms of regional measurements, due to our strong *a priori* hypotheses, we only focused on bilateral temporo-occipital regions such as the fusiform and lingual gyrus where the color and visual word form areas are located (Bartels & Zeki, 2000; Pernet *et al.*, 2005; Joseph *et al.*, 2006; Vinckier *et al.*, 2007). Differences between the two groups with respect to all regional anatomical measures, i.e. cortical thickness, volume and surface area as well as FA, were examined using *t*-tests with a height threshold of $P < 0.01$ uncorrected for multiple comparisons and an extent threshold of $k = 50$ vertices (and 30 voxels in the case of FA). For regions outside these areas we used a statistical threshold of $P < 0.05$ corrected for multiple comparisons. With respect to age, ICV and global anatomical measures, we used *t*-tests with a threshold of $P < 0.05$ uncorrected.

Results

Global measurements

As shown in Table 1 the left- and right-hemispheric cortical surface areas were slightly larger in synesthetes (left hemisphere, $t_{46} = 2.4$, $P = 0.021$; right hemisphere, $t_{46} = 2.25$, $P = 0.029$). We also found larger cortical volumes within the right hemisphere in synesthetes ($t_{46} = 2.22$, $P = 0.031$) and a trend toward significantly larger cortical volumes within the left hemisphere in synesthetes ($t_{46} = 1.79$, $P = 0.080$). There were no group differences with respect to age, cortical thickness, intracranial volume or mean fractional anisotropy.

Surface-based measurements

As shown in Fig. 1 and Table 2, we obtained larger cortical volumes and cortical thickness values in synesthetes than in non-synesthetes in several regions of the ventral visual stream including the right FG (Fig. 1C–E; location of peak difference for cortical volume: $x = 34$, $y = -34$, $z = -25$; and for cortical thickness: $x = 29$, $y = -50$, $z = -14$). Moreover, we revealed larger cortical surface area in synesthetes in the left FG (Fig. 1G; $x = -39$, $y = -38$, $z = -25$). There were also significant differences in the lingual gyrus (Figs 1A and B, cortical volume: $x = -18$, $y = -46$, $z = -5$; $x = 3$, $y = -69$, $z = 8$; Fig. 1E, cortical thickness: $x = 24$, $y = -51$, $z = -2$; Fig. 1F, cortical surface area: $x = 5$, $y = -76$, $z = 9$). Besides these differences in the brain areas of highest interest there were also some group

TABLE 1. Demographic characteristics and global morphological measurements of the left and right cortices in the synesthetes and non-synesthetes

Measure	Grapheme–color synesthetes	Control subjects	*P*-value*
SBM sample	(*n* = 24)	(*n* = 24)	(df = 46)
Age (years)	29.2 ± 10.1 (18.0–46.0)	27.3 ± 6.2 (18.0–42.0)	0.434
Volume (cm^3)			
Intracranial	1473.1 ± 163.4 (1285.9–1776.9)	1440.2 ± 108.5 (1274.9–1647.2)	0.416
Total L cortical	262.8 ± 27.8 (226.8–317.7)	250.4 ± 19.0 (215.8–286.3)	0.08
Total R cortical	260.0 ± 24.5 (229.0–320.5)	245.9 ± 19.0 (215.8–278.7)	0.031
Thickness (mm)			
Mean L cortical	2.618 ± 0.104 (2.380–2.780)	2.657 ± 0.083 (2.490–2.810)	0.162
Mean R cortical	2.606 ± 0.094 (2.440–2.800)	2.624 ± 0.070 (2.520–2.760)	0.47
Surface area (cm^2)			
Total L cortical	897.5 ± 90.7 (747.5–1052.7)	843.5 ± 62.4 (720.2–1006.9)	0.021
Total R cortical	894.7 ± 88.4 (759.5–1059.0)	842.9 ± 69.6 (715.6–1026.8)	0.029
DTI sample	(*n* = 14)	(*n* = 14)	(df = 26)
Age (years)	28.6 ± 7.6 (18.0–42.0)	29.4 ± 10.4 (18.0–46.0)	0.821
Fractional anisotropy (0–1)	0.261 ± 0.012 (0.233–0.279)	0.260 ± 0.083 (0.245–0.273)	0.806

Data are presented as Means ± SD, with range (minimum–maximum) in parentheses. SBM, surface-based morphometry; DTI, diffusion tensor imaging; FA, fractional anisotropy; L, left; R, right; df, degrees of freedom. **P*-value according to *t*-tests.

© The Authors (2009). Journal Compilation © Federation of European Neuroscience Societies and Blackwell Publishing Ltd

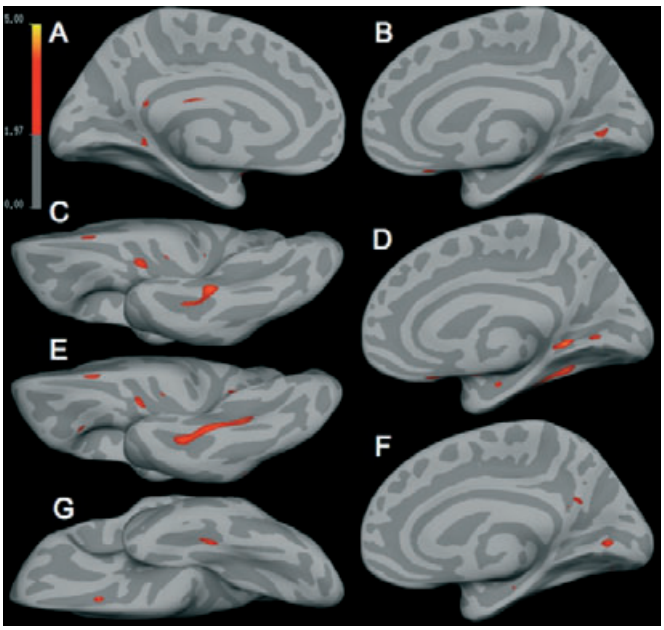

FIG. 1. Statistical parametric maps of the surface-based morphometry. Shown are predicted clusters of (A–C) increased cortical volume, (D and E) cortical thickness and (F and G) cortical surface area in the synesthetes compared with non-synesthetes in the fusiform, lingual and calcarine cortex (summarized in Table 2). Statistical parametric maps were projected onto the mean cortical surface of the 48 participants and thresholded with $P < 0.01$ uncorrected for multiple comparisons.

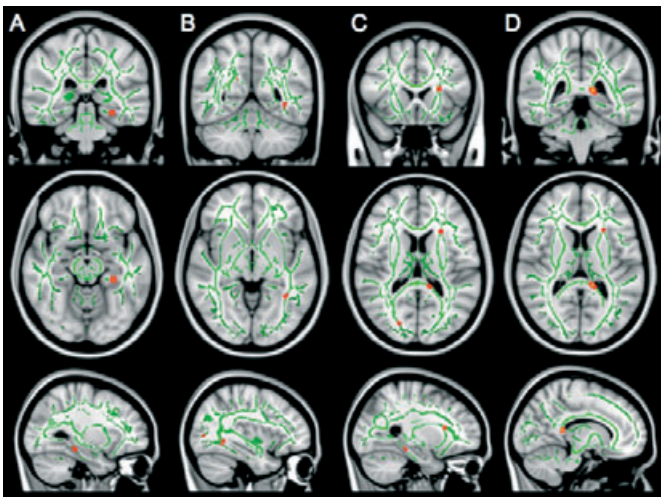

FIG. 2. Statistical parametric maps of the diffusion tensor imaging. Shown are regions with increased fractional anisotropy in the synesthetes compared with non- synesthetes in (A) the left hippocampus, (B) the left optic radiation, (C) the left inferior fronto-occipital fasciculus and (D) the splenium of the corpus callosum. Statistical parametric maps were overlaid on the mean structural image of the 48 participants and thresholded with $P < 0.01$ uncorrected for multiple comparisons. The skeleton of the mean fiber tracts is shown in green.

differences in adjacent brain regions, namely the calcarine cortex (Fig. 1D) and lateral occipital areas, with synesthetes showing larger values than controls. Applying the uncorrected statistical height threshold (which we used for the regions for which we have strong *a priori* hypotheses) there were also some morphological differences in areas for which we did not have *a priori* hypotheses. We present these brain areas in Table 3 because they can also be seen in the figures showing the morphological differences for which we had strong *a priori* hypotheses (Table 3). When using corrections for multiple comparisons for brain regions outside the temporo-occipital and visual cortex, there were no statistically significant differences in any of our morphometric measures. We did not assess the inverse contrast, i.e. regions where non-synesthetes showed larger values than synesthetes, because we had no *a priori* hypotheses.

FA measurements

Applying a statistical threshold of $P < 0.01$ (uncorrected for multiple comparisons), we did not find any significant differences between FA values in synesthetes and non-synesthetes in the ventral visual stream comprising the FG. Lowering the statistical threshold to $P = 0.05$ (uncorrected for multiple comparisons), we detected larger FA values

TABLE 2. Surface-based morphometry results: predicted clusters for synesthetes > controls

Measure and anatomical location	Figure	Hemi-sphere	Cluster size (mm^2)	Number of vertices	MNI coordinates			*P*-value (df = 45)
					x	*y*	*z*	
Cortical volume								
Calcarine sulcus/lingual gyrus	1A	Left	36.1	70	−18	−46	−5	0.0031
Lingual gyrus/intracalcarine								
cortex (V1)	1B	Right	74.8	105	3	−69	8	0.0034
Fusiform gyrus	1C	Right	183	281	34	−34	−25	0.0005
Cortical thickness								
Calcarine sulcus (V2)/lingual gyrus	1D, E	Right	148.9	334	24	−51	−2	0.0002
Intracalcarine cortex (V1)	1D	Right	79.5	86	5	−65	10	0.0011
Fusiform gyrus (anterior V4) extending into the anterior collateral transverse sulcus	1D, E	Right	419.6	622	29	−50	−14	0.0006
Lateral superior occipital cortex	(NS)	Right	72.5	85	45	−79	21	0.0042
Cortical surface area								
Fusiform gyrus	1G	Left	63.8	88	−39	−38	−25	0.0013
Lingual gyrus/intracalcarine cortex (V1)	1F	Right	99.4	106	5	−76	9	0.0018
Lateral occipital cortex	(NS)	Right	39.7	50	30	−86	7	0.0021
Precuneus	1F	Right	39.1	67	4	−59	27	0.0046

Predicted clusters of increased cortical volume, thickness and surface area in the synesthetes compared with non-synesthetes in the fusiform, lingual and calcarine cortex (as shown in Fig. 1). MNI, Montreal Neurological Institute; NS, not shown.

© The Authors (2009). Journal Compilation © Federation of European Neuroscience Societies and Blackwell Publishing Ltd

TABLE 3. Surface-based morphometry results: unexpected clusters for synesthetes > controls

Measure and anatomical location	Figure	Hemi-sphere	Cluster size (mm^2)	Number of vertices	MNI coordinates			*P*-value (df = 45)
					x	*y*	*z*	
Cortical volume								
Pericallosal sulcus	1A	Left	12	54	−9	−48	19	0.0052
Rectal gyrus	1B, C	Right	20.8	62	9	26	−22	0.0035
Cortical thickness								
Orbitofrontal cortex	1E	Left	112.1	267	−23	12	−23	0.0013
Central sulcus	NS	Right	107.9	182	48	−6	41	0.0008
Rectal gyrus	1E	Right	25.6	82	10	25	−25	0.0023
Middle temporal gyrus	NS	Right	69.8	107	68	−15	−19	0.0031
Postcentral gyrus	NS	Right	27.8	78	61	−10	40	0.0039
Superior circular sulcus of insula	NS	Right	51.1	112	46	−14	22	0.0042
Cortical surface area								
Cingulate gyrus (main part)	NS	Left	89	168	−6	20	29	0.0006
Superior circular sulcus of insula	NS	Left	25.9	62	−35	−14	20	0.0047
Inferior circular sulcus of insula	NS	Right	26.4	54	40	−11	−13	0.0027
Orbitofrontal cortex	1G	Right	74.4	78	25	54	−14	0.0049

Clusters of increased cortical volume, thickness and surface area in the synesthetes compared with non-synesthetes in brain regions that were not *a priori* expected (some of them are shown in Fig. 1). MNI, Montreal Neurological Institute.

TABLE 4. Diffusion tensor imaging results (fractional anisotropy): predicted clusters for synesthetes > contsrols

Anatomical location	Figure	Hemi-sphere	Cluster size (mm^2)	MNI coordinates			*P*-value (df = 26)
				x	*y*	*z*	
Hippocampus	2A	Left	70	−9	−33	−14	0.000051
Optic radiation/inferior fronto-occipital fasciculus	2B	Left	51	−35	−52	−4	0.000231
Inferior fronto-occipital fasciculus	2C	Left	49	−25	20	14	0.00041
Splenium of corpus callosum	2D	Left	34	−12	−40	11	0.000004

Listed are regions with increased fractional anisotropy in the synesthetes compared with non-synesthetes. MNI, Montreal Neurological Institute.

in synesthetes in left-sided fiber tracts in the FG. Using a height threshold of $P < 0.01$ (uncorrected for multiple comparisons) we found increased FA values in synesthetes (Table 4) in the hippocampus (Fig. 2A), the inferior fronto-occipital fasciculus (Figs 2B and C) and in the splenium of the corpus callosum (Fig. 2D). We did not assess the inverse contrast, i.e., regions where non-synesthetes showed larger FA values than synesthetes, because we had no *a priori* hypotheses.

Discussion

The aim of the present study was to establish the presence of neuroanatomical correlates of grapheme–color synesthesia in the ventral visual stream including the FG. As hypothesized, we found increased cortical volume, cortical thickness and cortical surface areas in synesthetes than in non-synesthetes. Differences in cortical structure were most prominent in the more anterior parts of the FG, roughly in the area of V4α, that is, in brain regions shown to be involved in color, letter and word processing (Bartels & Zeki, 2000; Pernet *et al.*, 2005; Joseph *et al.*, 2006; Vinckier *et al.*, 2007). These brain areas have also been identified in functional studies using functional magnetic resonance imaging and electrical tomography in which the cortical activations in grapheme–color and color–hearing synesthetes were explored (Nunn *et al.*, 2002; Hubbard & Ramachandran, 2005; Hubbard *et al.*, 2005a; Sperling *et al.*, 2006; Beeli *et al.*, 2008). While two of these functional studies reported increased activations bilaterally in V4, the other three studies found only left-hemispheric activations. It is currently unclear whether the different asymmetry patterns reflect different processing strategies.

Our study found larger cortical thickness and cortical volume in synesthetes within the right anterior FG, while cortical surface area was larger within the left anterior FG. As far as cortical thickness and cortical volume are concerned, these findings correspond closely with those of Weiss & Fink (2008), who found increased grey matter density in the right FG. However, the peak differences in our study were more anteriorly located than those of Weiss and Fink. The left anterior FG, for which we obtained larger cortical surface measures in synesthetes, has been shown to be involved in color naming (Chao & Martin, 1999). By lowering the statistical thresholds to a more lenient significance level of $P < 0.05$ (uncorrected) we also detected bilateral differences in the FG. However, by lowering the statistical threshold we did not find differences in the IPS and were therefore unable to replicate the findings of Weiss & Fink (2008), at least in the left IPS. Irrespective of these incongruencies, our findings do support the hypothesis of a different cortical structure in grapheme–color synesthetes in brain areas involved in color, letter and word processing.

Our DTI data only partially replicate previous findings of increased fractional anisotropy in the right ventral visual stream including the FG (Rouw & Scholte, 2007). Only by substantially lowering the statistical threshold ($P < 0.05$ uncorrected) were we able to detect differences in FA values between synesthetes and non-synesthetes in the right FG. It is of course clear that, at such a low threshold, the FA differences found in the FG bilaterally suffer a loss of specificity because many widely distributed brain areas also showed structural differences. We did uncover a correspondence between the peak difference for the cortical volume found in our study and the increased FA values found in the Rouw & Scholte (2007) study (Fig. 1C: 34,

© The Authors (2009). Journal Compilation © Federation of European Neuroscience Societies and Blackwell Publishing Ltd

−34, −25; Rouw & Scholte: 36, −40, −21). It remains to be established whether the discrepancy in findings is attributable to global inter-individual differences in cortical structures or different strategies of the synesthetes which might be related to differences in the underlying neuroanatomy (e.g. projecting or associating).

Cortical thickness (and cortical volume) as used in our study is a measure of the brain's outer surface, which contains ∼80% of neurons. Within this thin sheet, measuring only 1.5–4.5 mm, strong local connections (0–3 mm) between neurons are formed, thus promoting the idea of local processing units (small world networks). More remote connections are achieved via fibers in white matter tracts, as connections between either gyri, hemispheres, basal ganglia or other nuclei (e.g. thalamus). Increased cortical thickness (as in our study) could be due to a greater arborisation per neuron, increased glial volume or increased regional vasculature. Our findings may therefore be taken to suggest that local processing units within the fusiform gyrus are differently organized in grapheme–color synesthesia. However, future studies have to explore whether local anatomical features evolve independently of connections between remote brain areas.

In addition to the differences in the FG, we detected different cortical morphometric measures in the precuneus, superior occipital cortex, orbitofrontal cortex, the vicinity of the central sulcus, the hippocampus and the insula. Given that effects were below the threshold of corrected significance, and that we did not have any *a priori* hypothesis for these particular brain regions, these data need to be viewed with due caution. Future analyses are clearly necessary to confirm the significance of these regions before any sound conclusions can be drawn.

In summary, our study revealed structural alterations in cortical volume, cortical thickness and cortical surface area associated with grapheme–color synesthesia in the ventral visual stream including the FG. This leads to the suggestion that the specific interlinkage between graphemes and color in synesthetes is causally attributable to these specific anatomical alterations. However, great caution is due when drawing conclusions on the basis of anatomical differences between synesthetes and non-synesthetes. First, although all published morphometric studies of grapheme–color synesthetes have uncovered similarities, there are striking differences between these studies. It follows from this that the evident (and partly diverging) anatomical differences cannot entirely explain grapheme–color synesthesia. Secondly, the anatomical findings are not entirely compatible with the 'cortical disinhibition' hypotheses (Grossenbacher & Lovelace, 2001; Cohen Kadosh & Henik, 2007). Finally and most importantly, it is possible that the detected anatomical differences are a consequence of and not the primary reason for the life-long experience of grapheme–color synesthesia. Several studies have shown that short- and long-term motor and cognitive training is associated with selective and transient neuroanatomical changes in grey and white brain matter in young and older subjects (Draganski *et al.*, 2004, 2006, 2008; Boyke *et al.*, 2008; Driemeyer *et al.*, 2008). The amount of practice is also known to be an important factor in defining the extent of anatomical reorganizations (Maguire *et al.*, 2000; Gaser & Schlaug, 2003; Bengtsson *et al.*, 2005; Aydin *et al.*, 2007; Cannonieri *et al.*, 2007).

Acknowledgements

During the preparation of this manuscript J.H. and L.J. were supported by the Swiss National Science Foundation [National Centers of Competence in Research (NCCR): 'Neural Plasticity and Repair']. We thank Marcus Cheetham for improving the English of this manuscript.

Abbreviations

DTI, diffusion tensor imaging; FA, fractional anisotropy; FG, fusiform gyrus; IPS, intraparietal sulcus.

References

Annett, M.A. (1970) A classification of hand preference by association analysis. *Br. J. Psychol.*, **61**, 303–321.

Aydin, K., Ucar, A., Oguz, K.K., Okur, O.O., Agayev, A., Unal, Z., Yilmaz, S. & Ozturk, C. (2007) Increased gray matter density in the parietal cortex of mathematicians: a voxel-based morphometry study. *AJNR Am. J. Neuroradiol.*, **28**, 1859–1864.

Baron-Cohen, S., Wyke, M.A. & Binnie, C. (1987) Hearing words and seeing colours: an experimental investigation of a case of synaesthesia. *Perception*, **16**, 761–767.

Bartels, A. & Zeki, S. (2000) The architecture of the colour centre in the human visual brain: new results and a review. *Eur. J. Neurosci.*, **12**, 172–193.

Beeli, G., Esslen, M. & Jancke, L. (2007) Frequency correlates in Grapheme–color synaesthesia. *Psychol. Sci.*, **18**, 5.

Beeli, G., Esslen, M. & Jancke, L. (2008) Time course of neural activity correlated with colored-hearing synesthesia. *Cereb. Cortex*, **18**, 379–385.

Behrens, T.E.J., Woolrich, M.W., Jenkinson, M., Johansen-Berg, H., Nunes, R.G., Clare, S., Matthews, P.M., Brady, J.M. & Smith, S.M. (2003) Characterization and propagation of uncertainty in diffusion-weighted MR imaging. *Magn. Reson. Med.*, **50**, 1077–1088.

Bengtsson, S.L., Nagy, Z., Skare, S., Forsman, L., Forssberg, H. & Ullen, F. (2005) Extensive piano practicing has regionally specific effects on white matter development. *Nat. Neurosci.*, **8**, 1148–1150.

Boyke, J., Driemeyer, J., Gaser, C., Buchel, C. & May, A. (2008) Training-induced brain structure changes in the elderly. *J. Neurosci.*, **28**, 7031–7035.

Cannonieri, G.C., Bonilha, L., Fernandes, P.T., Cendes, F. & Li, L.M. (2007) Practice and perfect: length of training and structural brain changes in experienced typists. *Neuroreport*, **18**, 1063–1066.

Chao, L.L. & Martin, A. (1999) Cortical regions associated with perceiving, naming, and knowing about colors. *J. Cogn. Neurosci.*, **11**, 25–35.

Cohen Kadosh, R. & Henik, A. (2007) Can synaesthesia research inform cognitive science? *Trends Cogn. Sci.*, **11**, 177–184.

Dale, A.M., Fischl, B. & Sereno, M.I. (1999) Cortical surface-based analysis: I. segmentation and surface reconstruction. *NeuroImage*, **9**, 179–194.

Desikan, R.S., Ségonne, F., Fischl, B., Quinn, B.T., Dickerson, B.C., Blacker, D., Buckner, R.L., Dale, A.M., Maguire, R.P., Hyman, B.T., Albert, M.S. & Killiany, R.J. (2006) An automated labeling system for subdividing the human cerebral cortex on MRI scans into gyral based regions of interest. *NeuroImage*, **31**, 968–980.

Draganski, B., Gaser, C., Busch, V., Schuierer, G., Bogdahn, U. & May, A. (2004) Neuroplasticity: changes in grey matter induced by training. *Nature*, **427**, 311–312.

Draganski, B., Gaser, C., Kempermann, G., Kuhn, H.G., Winkler, J., Buchel, C. & May, A. (2006) Temporal and spatial dynamics of brain structure changes during extensive learning. *J. Neurosci.*, **26**, 6314–6317.

Draganski, B., Kherif, F., Kloppel, S., Cook, P.A., Alexander, D.C., Parker, G.J.M., Deichmann, R., Ashburner, J. & Frackowiak, R.S.J. (2008) Evidence for segregated and integrative connectivity patterns in the human basal ganglia. *J. Neurosci.*, **28**, 7143–7152.

Driemeyer, J., Boyke, J., Gaser, C., Büchel, C. & May, A. (2008) Changes in gray matter induced by learning – revisited. *PLoS ONE*, **3**, e2669.

Esterman, M., Verstynen, T., Ivry, R.B. & Robertson, L.C. (2006) Coming unbound: disrupting automatic integration of synesthetic color and graphemes by transcranial magnetic stimulation of the right parietal lobe. *J Cogn Neurosci*, **18**, 1570–1576.

Fischl, B. & Dale, A.M. (2000) Measuring the thickness of the human cerebral cortex from magnetic resonance images. *Proc. Natl Acad. Sci. USA*, **97**, 11050–11055.

Fischl, B., Sereno, M.I. & Dale, A.M. (1999a) Cortical surface-based analysis: ii: inflation, flattening, and a surface-based coordinate system. *NeuroImage*, **9**, 195–207.

Fischl, B., Sereno, M.I., Tootell, R.B.H. & Dale, A.M. (1999b) High-resolution intersubject averaging and a coordinate system for the cortical surface. *Hum. Brain Mapp.*, **8**, 272–284.

Fischl, B., Liu, A. & Dale, A.M. (2001) Automated manifold surgery: constructing geometrically accurate and topologically correct

© The Authors (2009). Journal Compilation © Federation of European Neuroscience Societies and Blackwell Publishing Ltd

models of the human cerebral cortex. *IEEE Trans. Med. Imaging*, **20**, 70–80.
Fischl, B., Salat, D.H., Busa, E., Albert, M., Dieterich, M., Haselgrove, C., van der Kouwe, A., Killiany, R., Kennedy, D., Klaveness, S., Montillo, A., Makris, N., Rosen, B. & Dale, A.M. (2002) Whole brain segmentation: automated labeling of neuroanatomical structures in the human brain. *Neuron*, **33**, 341–355.
Fischl, B., Salat, D.H., van der Kouwe, A.J.W., Makris, N., Segonne, F., Quinn, B.T. & Dale, A.M. (2004a) Sequence-independent segmentation of magnetic resonance images. *NeuroImage*, **23**, S69–S84.
Fischl, B., van der Kouwe, A., Destrieux, C., Halgren, E., Segonne, F., Salat, D.H., Busa, E., Seidman, L.J., Goldstein, J., Kennedy, D., Caviness, V., Makris, N., Rosen, B. & Dale, A.M. (2004b) Automatically parcellating the human cerebral cortex. *Cereb. Cortex*, **14**, 11–22.
Gaser, C. & Schlaug, G. (2003) Brain structures differ between musicians and non-musicians. *J. Neurosci.*, **23**, 9240–9245.
Grossenbacher, P.G. & Lovelace, C.T. (2001) Mechanisms of synesthesia: cognitive and physiological constraints. *Trends Cogn. Sci.*, **5**, 36–41.
Hänggi, J., Beeli, G., Oechslin, M.S. & Jäncke, L. (2008) The multiple synaesthete E.S. – Neuroanatomical basis of interval-taste and tone-colour synaesthesia. *NeuroImage*, **43**, 192–203.
Hubbard, E.M. (2007) Neurophysiology of Synesthesia. *Curr. Psychiatry Rep.*, **9**, 193–199.
Hubbard, E.M. & Ramachandran, V.S. (2005) Neurocognitive mechanisms of synesthesia. *Neuron*, **48**, 509–520.
Hubbard, E.M., Arman, A.C., Ramachandran, V.S. & Boynton, G.M. (2005a) Individual differences among grapheme–color synesthetes: brain-behavior correlations. *Neuron*, **45**, 975–985.
Hubbard, E.M., Piazza, M., Pinel, P. & Dehaene, S. (2005b) Interactions between number and space in parietal cortex. *Nat. Rev. Neurosci.*, **6**, 435–448.
Joseph, J.E., Cerullo, M.A., Farley, A.B., Steinmetz, N.A. & Mier, C.R. (2006) fMRI correlates of cortical specialization and generalization for letter processing. *NeuroImage*, **32**, 806–820.
Kuperberg, G.R., Broome, M.R., McGuire, P.K., David, A.S., Eddy, M., Ozawa, F., Goff, D., West, W.C., Williams, S.C.R., van der Kouwe, A.J.W., Salat, D.H., Dale, A.M. & Fischl, B. (2003) Regionally localized thinning of the cerebral cortex in schizophrenia. *Arch. Gen. Psychiatry*, **60**, 878–888.
Maguire, E.A., Gadian, D.G., Johnsrude, I.S., Good, C.D., Ashburner, J., Frackowiak, R.S.J. & Frith, C.D. (2000) Navigation-related structural change in the hippocampi of taxi drivers. *Proc. Natl Acad. Sci. USA*, **97**, 4398–4403.
Muggleton, N., Tsakanikos, E., Walsh, V. & Ward, J. (2007) Disruption of synaesthesia following TMS of the right posterior parietal cortex. *Neuropsychologia*, **45**, 1582–1585.
Nunn, J.A., Gregory, L.J., Brammer, M., Williams, S.C., Parslow, D.M., Morgan, M.J., Morris, R.G., Bullmore, E.T., Baron-Cohen, S. & Gray, J.A. (2002) Functional magnetic resonance imaging of synesthesia: activation of V4/V8 by spoken words. *Nat. Neurosci.*, **5**, 371–375.
Pernet, C., Celsis, P. & Démonet, J.-F. (2005) Selective response to letter categorization within the left fusiform gyrus. *NeuroImage*, **28**, 738–744.
Rauch, S.L., Wright, C.I., Martis, B., Busa, E., McMullin, K.G., Shin, L.M., Dale, A.M. & Fischl, B. (2004) A magnetic resonance imaging study of cortical thickness in animal phobia. *Biol. Psychiatry*, **55**, 946–952.
Rich, A.N. & Mattingley, J.B. (2002) Anomalous perception in synaesthesia: a cognitive neuroscience perspective. *Nat.Rev.Neurosci.*, **3**, 43–52.
Rich, A.N., Bradshaw, J.L. & Mattingley, J.B. (2005) A systematic, large-scale study of synaesthesia: implications for the role of early experience in lexical-colour associations. *Cognition*, **98**, 53–84.
Rosas, H.D., Liu, A.K., Hersch, S., Glessner, M., Ferrante, R.J., Salat, D.H., van der Kouwe, A., Jenkins, B.G., Dale, A.M. & Fischl, B. (2002) Regional and progressive thinning of the cortical ribbon in Huntington's disease. *Neurology*, **58**, 695–701.
Rouw, R. & Scholte, H.S. (2007) Increased structural connectivity in grapheme–color synesthesia. *Nat. Neurosci.*, **10**, 792–797.
Salat, D.H., Buckner, R.L., Snyder, A.Z., Greve, D.N., Desikan, R.S.R., Busa, E., Morris, J.C., Dale, A.M. & Fischl, B. (2004) Thinning of the cerebral cortex in aging. *Cereb. Cortex*, **14**, 721–730.
Ségonne, F., Dale, A.M., Busa, E., Glessner, M., Salat, D., Hahn, H.K. & Fischl, B. (2004) A hybrid approach to the skull stripping problem in MRI. *NeuroImage*, **22**, 1060–1075.
Smith, S.M., Jenkinson, M., Woolrich, M.W., Beckmann, C.F., Behrens, T.E.J., Johansen-Berg, H., Bannister, P.R., De Luca, M., Drobnjak, I., Flitney, D.E., Niazy, R.K., Saunders, J., Vickers, J., Zhang, Y., De Stefano, N., Brady, J.M. & Matthews, P.M. (2004) Advances in functional and structural MR image analysis and implementation as FSL. *NeuroImage*, **23**, S208–S219.
Smith, S.M., Jenkinson, M., Johansen-Berg, H., Rueckert, D., Nichols, T.E., Mackay, C.E., Watkins, K.E., Ciccarelli, O., Cader, M.Z., Matthews, P.M. & Behrens, T.E.J. (2006) Tract-based spatial statistics: voxelwise analysis of multi-subject diffusion data. *NeuroImage*, **31**, 1487–1505.
Sperling, J.M., Prvulovic, D., Linden, D.E., Singer, W. & Stirn, A. (2006) Neuronal correlates of colour-graphemic synaesthesia: a fMRI study. *Cortex*, **42**, 295–303.
Vinckier, F., Dehaene, S., Jobert, A., Dubus, J.P., Sigman, M. & Cohen, L. (2007) Hierarchical coding of letter strings in the ventral stream: dissecting the inner organization of the visual word-form system. *Neuron*, **55**, 143–156.
Weiss, P.H. & Fink, G.R. (2008) Grapheme-colour synaesthetes show increased grey matter volumes of parietal and fusiform cortex. *Brain*, **132(Pt1)**, 65–70.
Weiss, P.H., Zilles, K. & Fink, G.R. (2005) When visual perception causes feeling: enhanced cross-modal processing in grapheme–color synesthesia. *NeuroImage*, **28**, 859–868.

© The Authors (2009). Journal Compilation © Federation of European Neuroscience Societies and Blackwell Publishing Ltd

Copyright of European Journal of Neuroscience is the property of Blackwell Publishing Limited and its content may not be copied or emailed to multiple sites or posted to a listserv without the copyright holder's express written permission. However, users may print, download, or email articles for individual use.